Partition Coefficients and the Free Energy of Confinement from Simulations of Nonideal Polymer Systems

Peter Cifra and Tomáš Bleha*

Polymer Institute, Slovak Academy of Sciences, 842 36 Bratislava, Slovakia

Received June 1, 2000; Revised Manuscript Received November 17, 2000

ABSTRACT: The investigation of the partitioning equilibrium in real polymer systems by Monte Carlo (MC) simulations is reported. In contrast to ideal chain treatments the factors such as flexibility and excluded volume in real chains, the finite concentration of macromolecules ϕ, and polymer adsorption on pore walls of the attractive strength ϵ_w are considered in computations. The free energy change $\Delta A/kT$ due to chain confinement in slitlike structures under nonideal conditions is estimated from simulations. The dependencies of the partition coefficient K on λ, the solute to pore size ratio, relevant to the static partitioning and to size exclusion chromatography (SEC), were computed. In all cases the factors considered enhance the partition coefficient K for a given λ and lead to more gradual changes of K with λ; i.e., the resolving power of the nonideal partitioning decreases relative to a case of ideal chain partitioning. The concentration effect on the steric partitioning coefficient K was found to depend markedly on the solvent quality in dilute solutions. In mixed-mode partitioning by a combination of steric exclusion and adsorption, the function $K(\lambda,\epsilon_w)$ is computed by a fit of the simulation data. This function properly reproduces for nonideal chains all liquid chromatography regimes, including the critical chromatography. An interpretation of the free energy changes $\Delta A/kT$ in nonideal partitioning, based on the loss of conformational and orientational entropies of coils on their confinement, is discussed.

Introduction

The partitioning of macromolecular solutes between small pores and bulk solution underlies various chromatographic and membrane separation processes. This phenomenon is characterized by the partition coefficient, K, which is the pore-to-bulk concentration ratio at equilibrium. The theoretical models of partitioning of flexible macromolecules were recently reviewed.[1] In earlier treatments the pure steric exclusion of ideal chains in infinitely dilute solutions was addressed. The analytical approach based on the analogy between diffusional motion of a particle and conformation of a freely jointed polymer chain provided[2,3] the relations for the partition coefficient K in the form of infinite series. The coefficient K was expressed as a function of the coil-to-pore size ratio $\lambda = R_g/D_p$, where R_g is the radius of gyration of a chain and D_p is a characteristic dimension of a pore. According to these relations, the coefficient K depends on the ratio λ only and not on each of these two parameters taken separately. K is related to the free energy of confinement $\Delta A = -kT \ln K$, which represents a penalty for the transfer of a molecule from the bulk solution to the pore. The specific expressions K vs λ or ΔA vs λ were derived[1−3] for various confining geometries such as a slit, a cylinder, or a sphere and various chain architectures.

Casassa's explicit partitioning rules[2,3] for flexible chains helped particularly in the rationalization of measurements of partitioning equilibrium of flexible polymers under static or dynamic (chromatographic) conditions. The dependence of K on the chain length N (molecular weight M) of a polymer is of primary interest in these methods. The steric interactions of a macromolecule and a pore usually dominate in the separation mechanism in the size exclusion chromatography (SEC). The partitioning in SEC occurs in the region where pore size is larger than the size of the solute. In typical SEC the partition coefficient K of flexible polymers decreases with increasing molecular size of macromolecules. Additionally, the analytical relations for ideal chains due to Casassa et al. are widely used[4−6] to estimate the reduction of the free energy ΔA of chains confined in various nanostructural elements such as interlamellar layers in semicrystalline polymers, lamellar domains in block copolymers, in intercalates and inclusion compounds, in latex particles, etc.

In real systems, for example in separation and transport of polymers, additional factors, not accounted for in the ideal chain treatment, have to be considered in thermodynamic analysis of confined macromolecules. These factors, which may modify the Casassa partitioning rules, include the finite length of chains and their polydispersity, chain flexibility, intrachain excluded volume and quality of solvent, solute concentration, polymer−wall interaction, the distribution of pore sizes and shapes, etc. Some of the parameters mentioned above were already considered in the analytical theory, measurements, or computer simulations of polymer partitioning.[7−20] For example, the treatment of the freely jointed chains of the variable segment length l_K has shown[7] that ideal chain partitioning relations are obeyed only at an infinitely small length l_K. The influence of the solvent quality on the partitioning function K vs λ was investigated by Monte Carlo (MC) simulations in a cubic pore.[8]

The thermodynamics of macromolecular partitioning can be substantially affected by attractive interaction between macromolecules and pore walls. To this end, the diffusion-equation theory of Casassa for the ideal chains was extended[9−11] to include a short-range adsorption potential, and the equation was solved for various combinations of the molecule-to-pore size ratio λ and the adsorption strength. The partition coefficients K for ideal linear and cyclic chains in the various

* Corresponding author. e-mail: upoltble@savba.sk.

10.1021/ma000964a CCC: $20.00 © 2001 American Chemical Society
Published on Web 01/05/2001

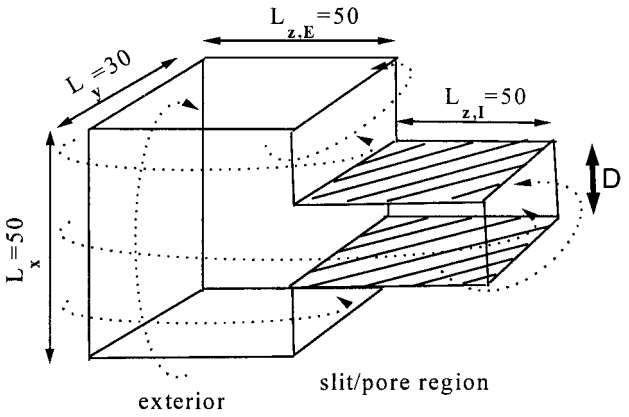

Figure 1. A sketch of the simulation setup. The slit width is denoted by D, and periodic boundary conditions are indicated by arrows.

regimes of narrow and broad pores were expressed[9,10] as a function of three parameters: R_g, D_p, and H, where H, the correlation length of adsorption, is proportional to the adsorbed layer thickness. Adsorption interactions are fundamental for liquid adsorption chromatography of macromolecules; to some extent they also contribute to the separation mechanism in real SEC of macromolecules on porous carriers.

Concentration of solute is another important variable affecting the coefficient K in macromolecular partitioning. Measurements of polymer partitioning at static equilibrium[12−14] demonstrated that in good solvents the coefficient K increases with the bulk concentration ϕ. This type of enhancement of polymer partitioning has also been observed in MC simulations of macromolecules in simple pore geometries.[15−17] The statistical thermodynamics models[18−20] were developed in order to explain the deviation of K from its value in very dilute solution, K_0, in good solvents.

The previous simulations conducted by Wang and Teraoka[17] treated partitioning of semidilute athermal chains into a slit between two parallel repulsive walls. Evidently, the changes in the thermodynamic quality of solvent to the theta condition and inclusion of attractive polymer−pore interaction will affect the partitioning characteristics. Both these factors are considered in MC simulations of nonideal polymer partitioning reported in the present paper. By successive incorporation of these and other features of nonideal polymer partitioning into the simulation model, the appropriate variations of the free energy ΔA and the coefficient K with the coil-to-pore size ratio λ are predicted from the simulations. The computed thermodynamic functions lead to an enhancement of the nonideal polymer partitioning for a given λ relative to the ideal chain partitioning.

Simulation Model

The simulation procedure was described previously in our papers devoted to the size and dimensional anisotropy of confined chains[21,22] and to the modeling of critical chromatography conditions.[23] Following the approach of Wang and Teraoka,[17] two boxes connected to each other (Figure 1) are assumed in simulations on a cubic lattice: the box E, representing the exterior (bulk) phase, and the box I, representing the interior slitlike pore. The box E has the dimensions $50 \times 30 \times 50$ (in lattice units) along the x, y, and z directions, respectively. In the box I of the dimensions $(D + 1) \times 30 \times 50$ there are two solid walls at $x = 1$ and at $x = D + 1$ extending in the y and z directions and forming a slit. The variable D is defined as the distance between the lattice layers occupied by the walls and is measured in lattice units. The polymer beads are not allowed to occupy the sites on the walls. Periodic boundary conditions apply with respect to all opposite walls in boxes except solid walls.

The self-avoiding walks (SAW) of the length N of 100 beads in the chain were generated on a cubic lattice in two solvent regimes. The athermal model of zero value of the reduced energy $\epsilon_s = e_s/kT$ of intrachain segment−segment contacts represented good solvents. The restrictions on the chain conformations imposed by the lattice occupancy bring about the volume expansion of chains similar to good solvents. The theta chains were generated using the reduced attractive energy[24,25] $\epsilon_s = -0.2693$ for both intra- and intermolecular nonbonded contacts. This specification rests on the assumption that for a long polymer interactions between portions well separated along the chain are equivalent to interactions between distinct chains. Hence, self-attraction and repulsion come into balance at the same temperature as do interchain attraction and repulsion. In addition, the equivalence of this value of attractive energy from different definitions of the theta temperature, i.e., from single chain and multichain behavior, was recently shown by Panagiotopoulos et al.[25] An ideal chain behavior was modeled by the generation of random walks (RW) on a cubic lattice.

In some simulations short-range adsorption interaction was considered between polymer segments and wall sites separated by one lattice unit. The strength of the reduced attraction energy per segment $\epsilon_w = e_w/kT$, which is zero at pure steric exclusion, varied from 0.5 (enhanced segment−wall repulsion) up to −0.3, covering thus the region of weakly adsorbed chains. Variations of the reduced adsorption energy can be interchanged with the variations of temperature.

Chains were equilibrated using the reptation moves and the Metropolis algorithm. The simulations provide the equilibrium concentrations of chains exchanging between bulk and a pore without the necessity of calculations of the confinement free energy ΔA from respective chemical potentials. The ratio of the volume fractions of a polymer in the interior and exterior boxes at equilibrium, ϕ_I/ϕ_E, gives the coefficient K. The chains in intermediate positions with their parts located in both boxes E and I at equilibrium contribute all their segments either to the volume fraction ϕ_I or to ϕ_E, depending on where the majority of the chain segments along the z axis is located.

The root-mean-square radius of gyration $R_g = \langle R_g \rangle^{1/2}$ of the free unconfined chains at infinite dilution was determined by the standard procedure. Simulations were performed for slit widths D between 6 and 48. The coil-to-pore size ratio, expressed as $\lambda = 2R_g/D$ since $D_p = D/2$, varied between 0.2 and 1.8, and thus fully covered the regions of weak ($\lambda \ll 1$) and moderate (λ around 1) confinements. In simulations of the concentration effect on steric partitioning, the volume fractions ϕ_E (denoted henceforth as ϕ) up to 0.13 were assumed.

Results and Discussion

The relations for the free energy ΔA and the coefficient K in ideal chain partitioning[1−3,9] are derived for the random-flight chains composed of noninteracting

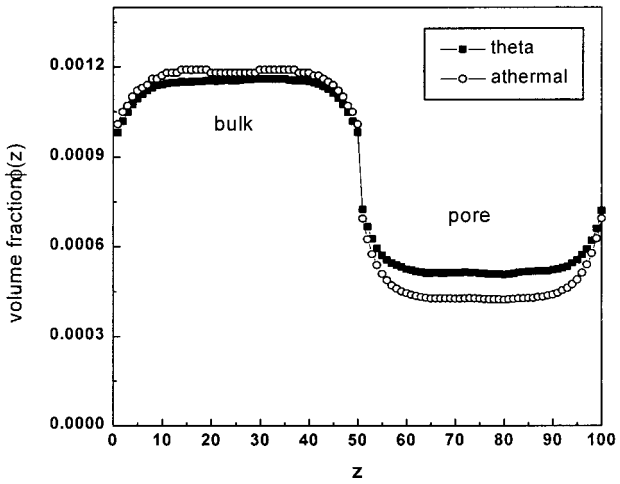

Figure 2. Transversal concentration profile $\phi(z)$ across the whole bulk-pore system along the axis z for slit of $D = 20$ at dilute athermal and Θ solutions. The average bulk concentration ϕ_E and the partition coefficient K are 0.001 16 and 0.384 and 0.001 13 and 0.467 for athermal and Θ systems, respectively.

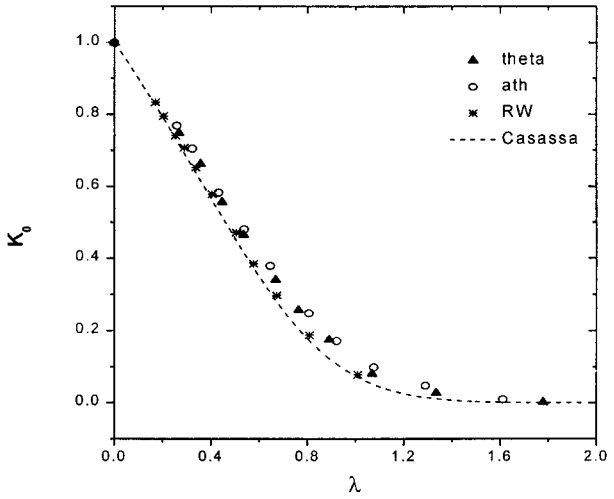

Figure 3. Variation of the partitioning coefficient K_0 as a function of the ratio $\lambda = 2R_g/D$ in a slit for SAW chains (athermal and Θ) and RW chains. Dashed line represents the results for ideal chains.[2,3]

segments. In the present approach these relations are modified by a successive incorporation of individual features of nonideal polymer partitioning such as excluded volume of chains, solute concentration, and polymer adsorption into the simulation model. The resulting functions of the free energy ΔA and of the coefficient K on the ratio λ should serve as a replacement of the respective ideal chain functions.

However, prior to presentation of the thermodynamic functions of partitioning, some information on the distribution of monomer density along the z-axis of the system bulk/pore shown in Figure 1 is worth mentioning. Particularly, the question arises whether the entrance region of a slit has properties much different from the pore interior region and in this way influences the partitioning results. To evaluate the pore entrance effects, we have calculated the transversal concentration profiles $\phi(z)$ across the whole bulk-pore system. The slit length along the z-axis assumed in the simulation model (50 lattice units) is a few times greater than the coil radius. The results for a slit of width $D = 20$ in dilute athermal and theta solutions are shown in Figure 2. The profiles are fairly flat in most of the bulk and pore regions, and the entrance effects are small.

Steric Partitioning of Nonideal Macromolecules. The properties of real chains are influenced by parameters such as the chain length N, the length of statistical (Kuhn) segment l_K (related to the chain flexibility), intramolecular excluded volume, etc. These and similar characteristics of chain nonideality may affect the partitioning due to steric exclusion at infinite dilution. The partitioning function $K_0(\lambda)$ of theta and athermal SAW chains at infinite dilution in equilibrium with a slit are shown in Figure 3. Since the system was equilibrated by a sufficient number of reptation moves, the statistical uncertainty of the data is typically of the size of the point markers in Figure 3 and in subsequent graphs. The reference behavior of ideal (Gaussian) chains is represented in Figure 3 by the Casassa function,[2,3] which in the region $\lambda \ll 1$ predicts a linear decrease of K_0 with λ with the slope $-2/(\pi)^{1/2}$.

Theta and athermal chains seem to follow about the same dependence of K_0 on λ in Figure 3. This finding is related to the fact that a use of the relative variable λ, the coil-to-pore size ratio, gives a "master curve" character to such a plot of the partitioning data. Any variations of coils size (at a given D) due to the chain length or solvent quality are in this plot translated into the shifts along the partitioning curve. Thus, an increase of the chain length N in SAW simulations results in a shift to higher λ, in the long-chain limit corresponding to $K = 0$. The same reasoning applies to the coil changes due to coil expansion in good solvents. The suppression in variations of the solvent quality by using plots of the partitioning coefficient K_0 as a function of a relative parameter λ was observed earlier[8] in simulations of chains in a cubic pore.

The random walk (RW) simulation data excellently match the Casassa ideal chain function in Figure 3, as was already observed earlier.[26] However, it should be noted that the MC results for both theta and athermal SAW chains are systematically shifted in Figure 3 to the higher K for a given λ relative to those for the Gaussian chains. The same trend was discernible in our previous study[16] of shorter ($N = 20-60$) athermal chains in a cubic pore. In view of that, it was mentioned[1] that SAW chains enter the restricting geometry more easily than the Gaussian chains of the same λ (of the same R_g for a given slit width). However, one should bear in mind that a specific value of R_g is achieved in SAW by shorter chains than in RW.

The enhancement of partitioning of the real (SAW) chains relative to the ideal chains can alternatively be attributed either to the effect of excluded volume or to the restricted flexibility of real chains (the finite length of chain segments). The ideal chain partitioning theory[2,3] relies on the freely jointed model of a chain of infinite number of (Kuhn) chain segments N_K and/or vanishingly small mean length of segment l_K. In an earlier study,[7] a substantial increase of K_0 for a given λ was found with the increase of chain rigidity expressed either by the ratio l_K/D or by N_K. In the limit $N_K = 1$ the behavior governed by the partitioning relation for the rigid rods[27] was observed.

The reduced free energies of confinement $\Delta A_0/kT$ of ideal and excluded volume chains as a function of λ are compared in Figure 4. Evidently, the free energy penalty due to confinement is smaller for both athermal and theta chains than for ideal chains. In the strong

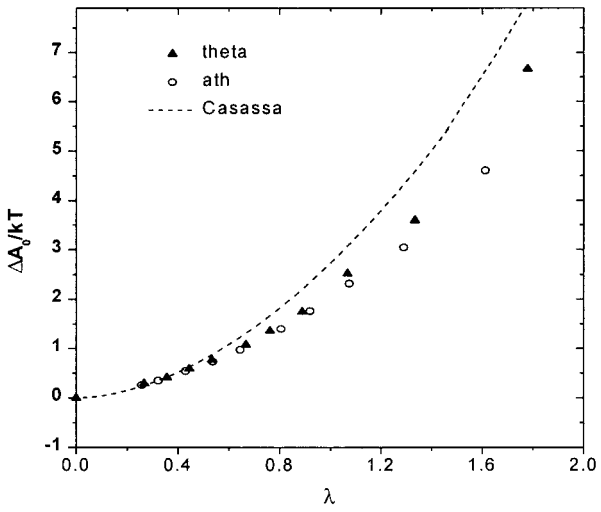

Figure 4. Free energy of confinement $\Delta A_0/kT = -\ln K$ of Θ and athermal chains as a function of the solute to pore size ratio λ. Dashed line represents the results for ideal chains.[2,3]

confinement regime $\lambda \gg 1$ (only partially covered by our simulations) the simple power law relation $\Delta A_0 \sim \alpha_1 \lambda^b$, where b depends on the solvent quality, was deduced from the scaling theory.[28,29] The exponents $b = 1.7$ and 2 were predicted[28] for good and Θ solvents, respectively. In harmony with the latter value of the exponent b, the free energy of confinement of ideal chains is proportional to λ^2 in the limit of long chains (or narrow pores).[1−3,9]

The MC data for athermal and theta chains in Figure 4 can formally be fitted by a power function

$$\Delta A_0/kT = p\lambda^q \tag{1}$$

inspired by the scaling theory, where p and q are adjustable parameters. Using the logarithmic form of the above function the linear fit of data in Figure 4 resulted in the following (p, q) parameters: (2.04, 1.57) for an athermal solvent and (2.17, 1.62) for a Θ solvent. Slightly higher exponents q were found by fitting the function in eq 1 directly by a nonlinear (allometric) fit. The fitting parameters above can be substituted into a stretched exponential $K_0 = \exp(-p\lambda^q)$ in order to represent the partitioning function $K_0(\lambda)$ in Figure 3. The numerical relations deduced in this way exemplify the partitioning rules of nonideal polymer chains at purely steric partition at infinite dilution. In contrast to the Casassa function, based on the summation of terms in a series, the fitting function used above comprises just one effective exponential term.

It should be noted, however, that despite formal similarity to the scaling relation, the data in Figures 3 and 4 cover also the regions of weak and moderate confinements, i.e., the range of λ outside of applicability of the scaling theory of confined chains.[28] Clearly, the value of the parameters p and q depends on the range of λ covered by fitting. The exponents $q = 1.57$ and 1.62 found by fitting of athermal and theta chain data, respectively, suggest that the above-mentioned difference in behavior of confined theta and athermal chains predicted by the scaling theory becomes operational in narrow pores only. Actually, as the confinement is getting stronger ($\lambda > 1$), the pace of increase of the theta curve in Figure 4 becomes larger than that of the athermal one. When the Casassa ideal chain functions are formally fitted by the function eq 1 in the range of λ shown in Figures 3 and 4, the effective exponent q of about 1.8 results, i.e., also below the limit of $q = 2$ for narrow pores.

All the features of the partitioning function $K_0(\lambda)$, such as its sigmoidal or linear form in the region of wide pores and the steepness of the change of K_0 with λ, are transmitted into a related variation of the coefficient K_0 with the chain length N, $K_0(N) = \exp[-\Delta A_0(N)/kT]$. Actually, this dependence underlies the use of the partitioning techniques for separation of macromolecules according to relative molecular weight M. Hence, an estimation of the effective exponent x in the relation

$$\Delta A_0 \approx N^x \tag{2}$$

is desirable in all partitioning results. The ideal chain theory[1−3,9] predicts $x = 1$, a linear variation of ΔA_0 with N in the limit of the strong confinement. A dependence of the radius of gyration on the chain length is needed to establish the exponent x in real chains. In our case the simulations of athermal chains of lengths between 20 and 300 yield the relation $R_g = 0.413N^{0.597}$, in harmony with the scaling theory predictions[29] $R_g \approx N^\nu$, where the exponent ν should be 0.59 and 0.5 for the athermal and theta chains, respectively. By introducing the above relation into the free energy fit (eq 1, $p = 2.04$, $q = 1.57$) of the athermal chain data in Figure 4, the following function results: $\Delta A_0/kT = 0.843D^{-1.57}N^{0.94}$. Hence, the free energy of confinement of athermal chains is related to the chain length by the lower-than-linear dependence. In other words, the proportionality $K_0 \approx \exp(-N^{0.94})$ applies to the partition coefficient K_0 of athermal chains at infinite dilution under pure steric exclusion mechanism. Similarly, the exponent $x = 0.81$ in eq 2 can be deduced for the Θ solvents when the scaling exponent $\nu = 0.5$ is assumed. In general, any reduction of the effective exponent x brings about the reduction of the resolving power of macromolecular partitioning.

Steric Partitioning in Dilute Solutions. Measurements of polymer partitioning under static conditions[12−14] show that in good solvents the coefficient K increases with bulk concentration ϕ. The concentration effect on K is usually expressed by using the virial series

$$K = K_0(1 + \kappa_1\phi + \kappa_2\phi^2 ...) \tag{3}$$

The results of MC simulation in athermal solvent (Figure 5) confirm that an increase of bulk concentration enhances the penetration of molecules into a pore. In the region of very dilute solution the increase of K is approximately linear, in agreement with our previous simulations of shorter chains.[15,16] The concentrations in Figure 5 cover the regime of a dilute solution, below the onset of coil overlap at the critical concentration[17] $\phi^* = N/(\sqrt{2}R_g)^3 = 0.132$ for $N = 100$. The results in Figure 5 for the athermal solvent are in accord with the findings of a related study[17] focused on semidilute and concentrated solutions in slightly different range of pore widths.

In striking contrast to athermal chains, the negligible concentration effect on K is seen from the simulation data in a Θ solvent in dilute solution regime (Figure 5). Simulations thus predict that steric partitioning in dilute solutions is remarkably affected by the solvent quality. So far no measurements of static partitioning in Θ solvents were reported in the literature. However,

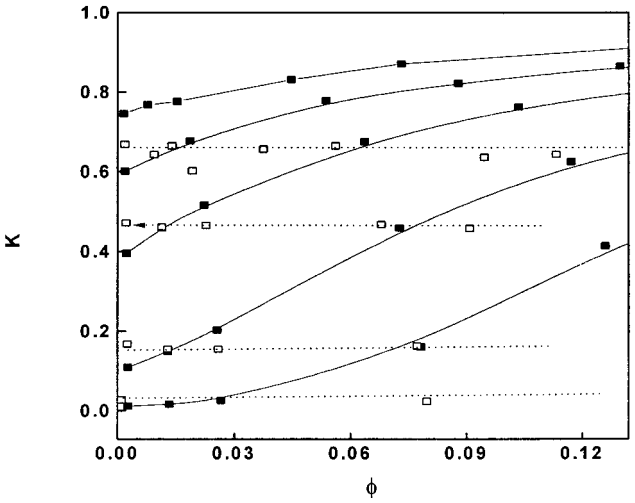

Figure 5. Dependence of partition coefficient K on bulk concentration ϕ for athermal chains (■, solid lines) and Θ chains (□, dotted lines) at various ratio λ (from the top): 0.28, 0.43, 0.65, 1.08, and 1.61 (athermal chains) and 0.36, 0.53, 0.89, and 1.33 (Θ chains).

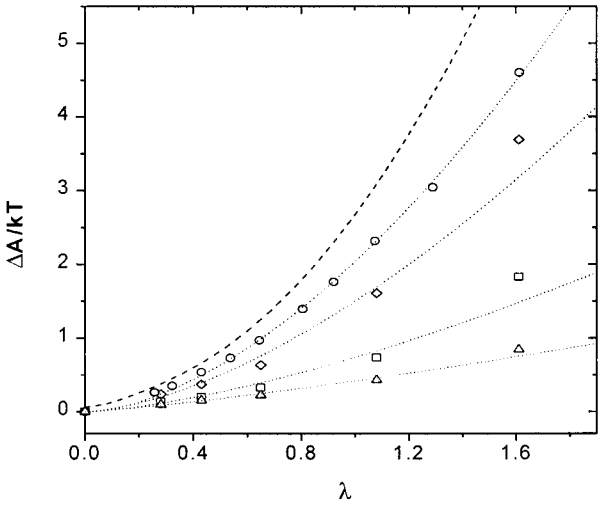

Figure 6. Free energy of confinement $\Delta A/kT$ of athermal chains as a function of the solute to pore size ratio λ for various relative concentration ϕ_{rel} (from the top): 0 (○), 0.19 (◇), 0.59 (□), 1 (△). Dotted lines show the linear fits of calculated data using the logarithmic form of eq 1. Dashed line presents the results for ideal chains.[2,3]

the concentration dependence of K can be inferred from the dynamic partitioning in SEC, specifically, from the shift of the peak elution volume V_e with the concentration c of the injected volume. Similarly to the data in Figure 5, a large concentration effect on V_e was observed in good solvents used as eluents, and a negligible effect was found in the Θ eluents.[30,31] From the measurements of the concentration effect in SEC in eluents of variable thermodynamic quality for injected polymers, a strong correlation was established[31,32] between the rate of increase of K with c and the product A_2M, where A_2 is the second osmotic virial coefficient. The simulation results in Figure 5 lend support to this correlation and confirm a common nature of the concentration effect in the static partitioning and in SEC. In both cases this phenomenon results primarily from deviations from ideality in bulk (external) solution that can be quantified by the term A_2M.

The detailed microscopic models[18−20] of the concentration effect in partitioning were later developed by quantification of polymer−polymer interaction and solution nonideality. The model of Teraoka et al.[19] is based on a equation of state from the renormalization group theory. A rigorous integral equation model was developed[20] for polymer solutions in the presence of rigid matrix of randomly placed obstacles. These models correctly predict the deviations of K according to eq 3 from its value in very dilute solutions K_0 in good solvents. The nonlinear partitioning of flexible macromolecules in nondilute athermal solutions can be related[19] to the osmotic pressure in the bulk solution of concentration ϕ. The osmotic pressure (polymer−polymer repulsion) drives the macromolecules (preferably shorter ones) into the pore and enhances the coefficient K.

The influence of concentration ϕ on the free energy of confinement $\Delta A/kT$ in athermal solutions is shown in Figure 6 for three relative concentrations $\phi_{rel} = \phi/\phi^*$. The term $\Delta A/kT$ represents the free energy of transfer of a molecule from bulk solution into a pore. The free energy penalty, already reduced in athermal solvent in infinite dilution relative to ideal chains, is further diminished by an increase of concentration ϕ. In the explanation of this trend, one should note that an

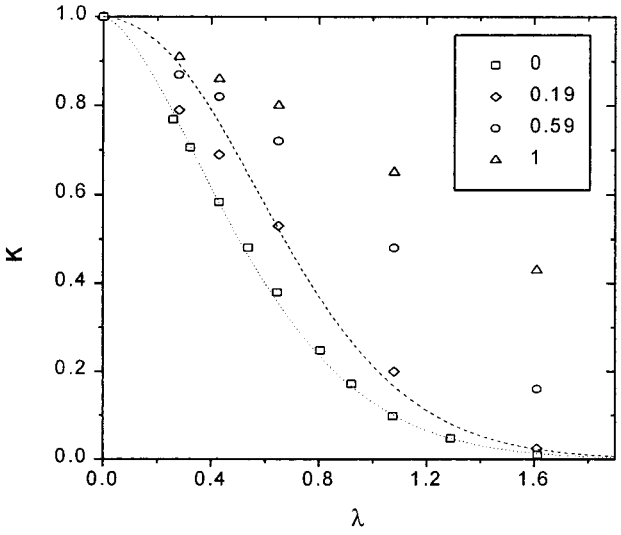

Figure 7. Partitioning curves K vs λ for indicated concentrations ϕ_{rel}. The dotted line correspond to a fit of infinite dilution data by eq 1. The dashed curve shows the prediction of the linear partitioning theory[19] for $\phi_{rel} = 0.19$.

increase of the polymer concentration ϕ in athermal solvent in bulk (external) phase diminishes the difference of logarithms of concentration in a pore interior and bulk, $\ln \phi_I - \ln \phi$, and the related difference of chemical potentials. It is evident from Figure 6 that the use of an ideal chain function to represent the term $\Delta A/kT$ at finite concentrations results in a considerable overestimate of the free energy penalty, particularly when the size of a solute and a slit becomes comparable.

Next, the effect of concentration on K from Figure 5 was incorporated into a partitioning curve $K(\lambda)$ in good solvents (Figure 7). An increase of the relative concentration ϕ_{rel} results here in a shift of the curves to the higher λ, and the partition curves become more flat. The MC data for $\phi_{rel} = 0.19$ in Figure 7 correspond to the region of linear partitioning at very dilute solutions in Figure 5 where the second and higher terms in the virial series can be neglected. Theoretical expressions[18,19] have been derived for the linear term k_1 in eq 3. The

corresponding function of Teraoka et al.[19] of the form $K = K_0[1 + 3.87(1 - K_0)\phi_{rel}]$ is plotted in Figure 7 for $\phi_{rel} = 0.19$. The agreement of the linear partitioning function with MC data in a slit is fairly good even though the above function was derived for a cylindrical pore.

In a treatment of steric partitioning as a function of two variables, λ and ϕ, a three-dimensional (3D) surface $K(\lambda,\phi)$ can be envisioned. Such a surface can be approximately constructed by using the logarithmic form of eq 1 to fit the free energy data in Figure 6. From these linear fits the following simple dependencies of parameters p and q on ϕ were found: $p = 2.04 - 2.42\phi_{rel} + 0.77\phi_{rel}^2$ and $q = 1.57 - 0.19\phi_{rel}$. The increased concentration reduces both parameters p and q from the values appropriate at infinite dilution. By the introduction of the above relations into eq 1 the surfaces $\Delta A/kT(\lambda,\phi)$ and $K(\lambda,\phi)$ were constructed (not shown). The $K(\lambda)$ curves in Figure 7 represent the sections though the surface $K(\lambda,\phi)$ for a given ϕ_{rel}. Alternative sections through this surface, the plots $K(\phi)$ for a given λ, correspond to the concentration functions in Figure 5.

The more gradual changes of K with λ at the finite concentration partitioning of athermal chains, noticeable in Figure 7, are an indication of a further reduction of the effective exponent x in eq 2 to values much below unity. This reduction of the exponent x at finite concentration can be tracked down to the osmotic pressure contribution to K, which in itself is also a function of N. For example, at $\phi_{rel} = 0.59$, the fit of the MC data in Figure 7 furnishes the exponent $q = 1.46$ in eq 1. Consequently, the exponent x in eq 2 equates in this case to 0.87, and the partitioning rule reads $K \approx \exp(-N^{0.87})$. The finite concentration reduces the exponent x relative to its value at infinite dilution; the resolving power of partitioning is diminished by concentration.

When the dependence $\Delta A/kT$ on N is stronger than linear, the steepness of the partitioning curve increases; i.e., the changes of λ in a narrow range are accompanied by considerable changes of K. Such type of the function $K(\lambda)$ was deduced from the dynamic partitioning of poly(ethylene oxide) (PEO) into the membrane-bound α-toxin pores.[33] The highly concentrated solutions (15% w/w) of PEO dissolved in H_2O with added salts were used in these experiments. By measurements of polymer-induced changes of the pore conductance in the range of M_{PEO} between 10^2 and 10^4, a sharp dependence of the coefficient K on M was observed. From the measured data the exponent $x = 3.1$ was derived for the chain length dependence of the free energy $\Delta A/kT$, eq 2. Accordingly, the free energy of confinement was found[33] to be proportional to the cube of the number of polymer segments.

Theories of partitioning[18−20] of hard spheres or flexible coils, including the scaling theory,[28] do not predict such sharp changes of the coefficient K with λ or N. The MC data on the concentration effect in Figure 7 show even the opposite trend, flattening of partitioning curves with increasing concentration instead of sharpening. The shape of the partitioning curves observed was interpreted in ref 33 by assuming the interaction between PEO and the surface of the pore which should attract the polymer molecule into the pore interior. The results of our simulations using a simple model of the polymer−pore adsorption (vide infra) are not in harmony with this suggestion; the partitioning curves become flatter by an increase of the adsorption strength. On the other hand, neither theory nor simulations cover such factors as hydrophobic interactions or the presence of electrolytes in a solution. The partitioning behavior of synthetic water-soluble polymers is frequently used in membrane techniques in an inverse manner to determine the size of protein ion conducting pores. Thus, a further examination of the above discrepancy between experimental results and predictions from theory and simulations is expedient.

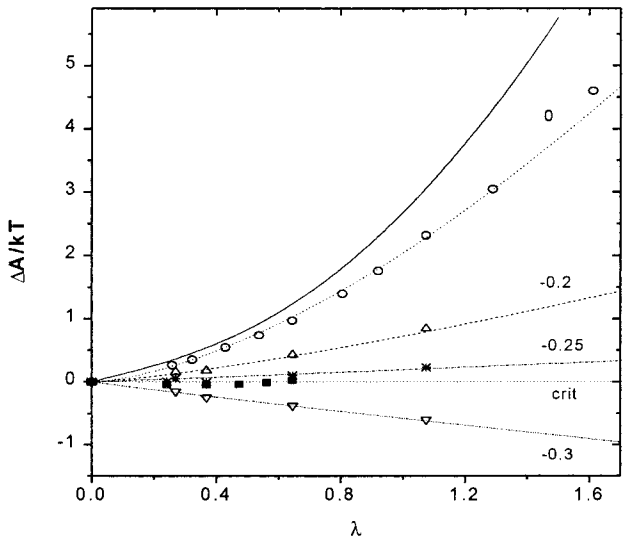

Figure 8. Free energy of confinement $\Delta A/kT$ of athermal chains as a function of the solute to pore size ratio λ for the indicated attraction strength ϵ_w. Dotted lines correspond to the linear fits of data using the logarithmic form of eq 1. The solid line represents the result for ideal chains.[2,3]

In contrast to good solvents, the single-chain functions of K_0 and $\Delta A_0/kT$ vs λ from Figures 3 and 4 for theta chains should be applicable at all concentrations in dilute solutions up to ϕ about 0.13, at least. It should be noted, however, that at very strong confinements the concept of the theta state is interconnected with the dimensionality of the system. It was noted[25] that the theta temperature is not the same in two and in three dimensions. At the theta temperature in 3D the second-order term in the expansion of polymer free energy vanishes, and a chain obeys the Gaussian statistics. However, in the 2D case, the chain is no longer ideal at the theta point. Hence, a chain originally in a poor solvent in 3D can be subjected to the whole range of solvent qualities when strongly confined, from poor to good solvents; the concentration effect on K can be influenced accordingly.

Partitioning by Steric Exclusion and Adsorption in Very Dilute Solutions. The adsorption of solute on the solid matrix such as column packing is frequently experienced in the partitioning of macromolecules. The mixed mode (steric exclusion/adsorption) mechanism of partitioning of real chains in good solvents at infinite dilution was simulated by an interplay of two potentials: (a) hard-core repulsion of chain segments on the lattice and (b) attraction between slit walls and the first-neighbor chain segments of the strength ϵ_w.

The mixed-mode partitioning data for the free energy of confinement $\Delta A/kT$ in athermal chains are plotted as a function of the ratio λ in Figure 8. The curve for $\epsilon_w = 0$ corresponds to a variation of $\Delta A_0/kT$ due to pure steric exclusion. The free energy of confinement is reduced by an increase in the polymer−pore attraction strength ϵ_w. Steric exclusion and adsorption effects in

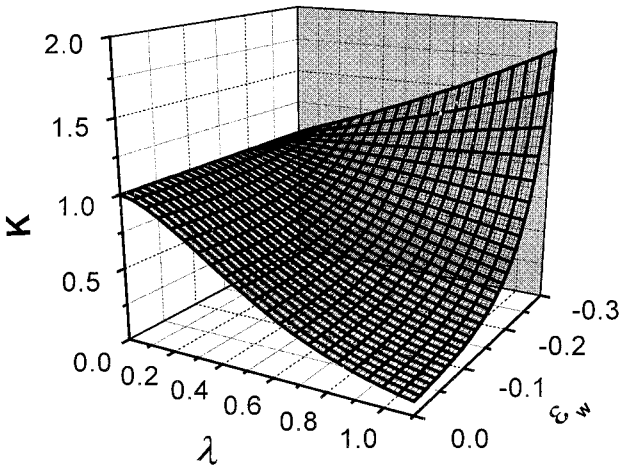

Figure 9. Partitioning coefficient K as a function of the ratio λ and attraction strength ϵ_w for athermal chains. The surface is constructed from the linear fit of simulation data by introduction of eq 4 into eq 1 (see text).

the partitioning are balanced at ϵ_w around -0.26. At the compensation point the free energy is zero (or $K = 1$), and the attraction strength ϵ_w* corresponds to the critical point of adsorption. Interestingly, at the attraction strengths higher than critical, a molecule in a pore becomes more stabilized than a molecule in the bulk phase, and this stabilization increases with confinement. Again, the data in Figure 8 were fitted using the logarithmic form of eq 1. It was found that the parameters p and q can be approximated by simple functions of ϵ_w:

$$p = 2.04 + 2.01\epsilon_w - 22.01\epsilon_w^2; \quad q = 1.57 + 2.17\epsilon_w \tag{4}$$

The fitting parameters at pure steric exclusion are reproduced by these equations. The increased attraction strength reduces both p and q: at the critical point $p = 0$ and $q = 1$.

The 3D surface $K(\lambda,\epsilon_w) = \exp(-\Delta A(\lambda,\epsilon_w)/kT)$, constructed for $\lambda < 1.1$ by a substitution of the above relations into eq 1, is shown in Figure 9. The changes in the partitioning of athermal chains due to variable wall attraction are readily seen from the 3D surface. The sections through the surface for a given ϵ_w furnish the partitioning curves[23] $K(\lambda)$ appropriate for a constant strength ϵ_w. Increasing attraction makes the curves $K(\lambda)$ at first to level off, and then above the critical attraction strength ϵ_w*, the coefficients K increase with λ for a given ϵ_w. In contrast, a very small modification of the reference curve $K_0(\lambda)$ was found by expanding ϵ_w from zero to positive values (repulsive pore walls). Alternative sections through the surface, the variations of K with ϵ_w at given λ, are presented in Figure 10. Here, the steepness of the curves $K(\epsilon_w)$ depends considerably on the λ selected. In a way, the functions $K(\epsilon_w)$ are an analogy to the concentration functions $K(\phi)$ plotted in Figure 5 and described by eq 3. The more gradual changes of K with λ by the mixed-mode partitioning of athermal chains shown in Figure 9 in the region between $\epsilon_w = 0$ and ϵ_w* suggest again a reduction of an effective exponent x in the dependence $\Delta A/kT$ on N to values much below unity. For example, the parameter $q = 1.30$ in eq 1 results from a linear fit of the data in Figure 8 for $\epsilon_w = -0.20$, and thus the exponent x in eq 2 is 0.78. Accordingly, pore attraction interaction in the

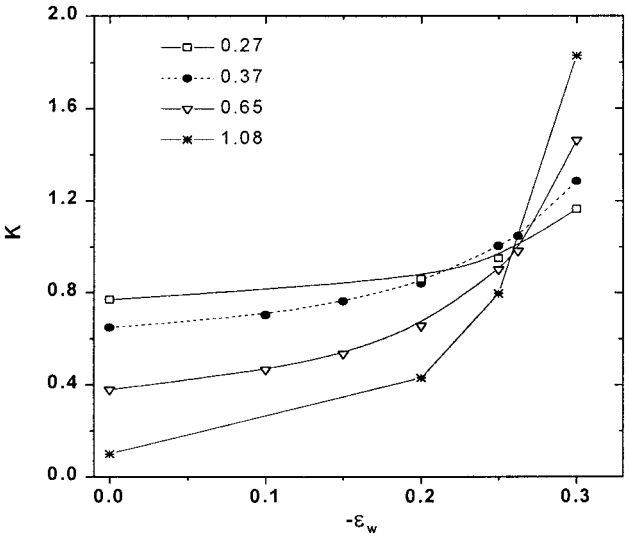

Figure 10. Plot of the coefficient K in athermal chains as a function of the attraction strength ϵ_w for indicated ratio λ as a parameter. The data for $\lambda = 0.37$ correspond to the chain length $N = 40$; all other data are for $N = 100$.

above region brings about the reduction of the resolving power of macromolecular partitioning, similar to the effect of concentration.

The differences in the adsorption energy of solutes are responsible for their separation in the liquid adsorption chromatography where $K > 1$. In real SEC of macromolecules on porous packings, the combined effect of steric exclusion and adsorption mechanisms is frequently operative. As shown in Figure 9, the different regimes of the steric exclusion/adsorption equilibrium in chromatography of real macromolecules are reproduced by the variation of the parameters λ and ϵ_w, including the region of the critical chromatography around $K(\lambda) = 1$. Since $K = 1$ at the compensation point, the exponent x in eq 2 is zero. This gives the possibility of selectively masking the component(s) in separations of complex systems by the critical chromatography.[34,35] The compensation point was predicted[36] to be independent of the chain length N for ideal chains, and thus the separation of solutes in critical chromatography should not be influenced by the molecular mass M of solute. However, in nonideal chains, the compensation point was found[23] to depend on the chain length (or M). In athermal chains of the length $N = 100$ in equilibrium with a slitlike pore with attractive walls the steric exclusion and adsorption effects fully compensate at ϵ_w* $= -0.2625$. Consequently, the shape of the surface $K(\lambda,\epsilon_w)$ in Figure 9 in the vicinity of $K = 1$ may be slightly affected by the chain length. This feature is also seen at the sections of this surface for a given λ in Figure 10. Since the 3D surface is constructed for the chain length $N = 100$, only the curves $K(\epsilon_w)$ pertaining to $N = 100$ intersect in Figure 10 at the critical value ϵ_w* $= -0.2625$.

Apart from small variations with N in the critical region, the function $K(\lambda,\epsilon_w)$, defined by eq 4 and obtained by a fit of the simulation data, should provide a fairly universal description of mixed-mode partitioning of nonideal chains. For a given ratio λ, specified by a molecular weight of a polymer and material porosity, the measured partition coefficient K should be a function of the parameter ϵ_w only. In the measurement of macromolecular partitioning the variation of the adsorption strength is usually realized by the change of

temperature or composition of the solvent. The attraction strength ϵ_w can be treated as an adjustable parameter to fit the experimental data.[37] The notion of universality of the function $K(\lambda,\epsilon_w)$ is supported by previous results using analytical theory[9,10] of ideal chains partitioning in the presence of attractive polymer−pore interaction. In this theory the partition coefficient K is expressed as a complex function of three parameters: R_g, D, and H. The correlation length of adsorption, H, is related to the attraction strength by the proportionality $H \approx l_K/(\epsilon_w^* - \epsilon_w)$. Thus, the ideal chain theory[9,10] employs essentially the same set of variables as that used in Figure 9. In the region of wide pores a relation was suggested[9] according to which in ideal chains the ratio $(K - K_0)/(1 - K_0)$ should depend solely on the ratio R_g/H. Chromatographic data of polymers at various temperatures and solvent mixtures endorse[9,37] the universal character of the proposed relation even in real polymers. The surface $K(\lambda,\epsilon_w)$ in Figure 9 represents an substitute to the mentioned universal relation in the case of nonideal chains and for much wider range of pores.

The Free Energy of Confinement. The term $\Delta A/kT$ plotted in Figures 4, 6, and 8 corresponds to the free energy of transfer of a molecule from bulk solution into a pore at equilibrium. This free energy penalty due to coil confinement is diminished by an increase of the concentration ϕ or adsorption strength. In the case of adsorption, in a regime above the critical point ϵ_w^*, the free energy of confinement is negative; the chains prefer the pore interior to the bulk phase. The deviations of the curves of $\Delta A/kT(\lambda)$ and $K(\lambda)$ in an athermal solvent from the reference ideal chain functions due to the concentration and adsorption effects presented in Figures 6−9 share many similar features; most prominently, in both cases the resolution power of nonideal partitioning is reduced. However, this qualitatively identical effect is achieved by completely different mechanisms. At finite concentrations repulsion between monomers (the osmotic pressure) in the bulk phase *pushes* chains into a pore. Interestingly, inclusion of attractive monomer−pore interaction acts in the same direction: attraction of walls *pulls* the chains into the pore. In both cases, despite the completely different nature of the driving force, the Casassa functions considerably overestimate $\Delta A/kT$ (underestimate the partition coefficient K), particularly when the solute and the pore are of comparable size. The difference between the free energy of confinement in ideal and nonideal partitioning represents several kT units. Thus, the utilization of the ideal chain expression to estimate an increase of the free energy ΔA of molecules confined in various nanosized structure elements might not be appropriate.

The steric free energy of confinement $\Delta A_0/kT$ at infinite dilution is intimately connected to the changes in the dimensions and in the shape of flexible macromolecules induced by the constraining geometry. These changes can be inferred from the MC simulations of single molecules confined in pores of a regular shape.[21,38] In an unconfined situation, single macromolecules shaped as cigars with an elliptic cross section are randomly oriented. At weak confinements in a slit, the dimensional changes of chains are minimal, and cigarlike molecules align along the pore walls. At moderate confinements (around $\lambda = 1$) molecules become squeezed along all three axes, and chain dimensions attain a minimum at their dependence on D.[21,22,38] Finally, at strong confinements (narrow pores) the coils are severely flattened into the quasi-two-dimensional disks. Qualitatively, all these features were also validated in the dilute and semidilute concentration regimes.[22,39]

From the variations of dimensions, shape, and anisotropy of confined macromolecules, two kinds of confinement-induced changes of entropy of coils can be inferred. First is the loss of conformational entropy ΔS_{conf} due to the rejection of conformations crossing the pore walls. This elimination of disallowed conformations actually corresponds to an effective modification of the instantaneous shape of cigarlike coils. The second mechanism,[39] the loss of orientational entropy ΔS_{or}, is effective at weak confinements. In contrast to a random orientation in the bulk phase, some orientations of cigarlike coils in a pore are not allowed due to steric exclusion of walls, and thus the molecules align along the pore walls.

These two entropy changes should affect the $\Delta A/kT$ term plotted in Figure 6 as a function of the concentration ϕ. Actually, the magnitude of both entropy factors diminishes at higher concentrations. For example, the calculation[39] of the orientational correlation function of molecular axis proved that the molecular axes are aligned parallel to the wall. The alignment decreased as the center of mass of a molecule moved away from the wall. As the concentration increased, the tendency for molecules to align along the wall was reduced. In the case of adsorption, an inclusion of the weak pore attraction produced no substantial changes in size and shape of confined macromolecules.[23] In this case, the free energy changes (Figure 8) are affected mainly by the enthalpy term ($\Delta H < 0$ due to attractive interaction) which reduces the free energy penalty. At the compensation point the loss of conformational and orientational entropy on confinement is fully balanced by the (adsorption) enthalpy gain. At the attraction strengths higher than critical, the term ΔH outweighs the entropy loss of a chain in a slit and ΔA becomes negative.

Finally, the impact of the results presented on the SEC calibration should be noted. The modification of partitioning curves due to concentration or adsorption is transmitted to the plot of log(hydrodynamic volume V_h) vs elution volume V_e. This function, denoted as the universal calibration and symbolizing the separation according to solute size, is frequently used to present data in SEC. The equation $V_e = V_0 + KV_I$ applies in SEC, where V_0 is the volume of the interstitial mobile phase and a V_I the volume of the quasi-stationary phase within the pores. For the fixed pore size the term log V_h is proportional to 3 log R_g. Hence, the term (3 log R_g + c), where c is a numerical constant, plotted as a function of K represents a variant of universal calibration. Using this plot, it was shown[40] that the universal calibration evaluated from real chain simulations at finite concentration or adsorption strengths is steeper and shifted to higher K relative to an analogous plot for "ideal" SEC based on pure steric exclusion. Again, it is a demonstration of the diminishing resolution power of SEC separation under nonideal conditions.

Conclusions

The individual factors in the nonideal partitioning of macromolecules were investigated by computer simulations. The new partitioning rules were established in three cases studied: (a) partitioning of single real chains

(as contrasted to ideal chains), (b) steric partitioning at finite polymer concentrations, and (c) adsorption of molecules on pore walls. The nonideal partitioning rules significantly deviate from the Casassa relation for ideal chains, and enhancement of the partitioning coefficient K for a given λ was experienced in all cases. A marked sensitivity of the concentration dependence of K to the solvent quality was found in steric partitioning in dilute solutions. The observed independence of the coefficient K from the concentration in Θ solvents is corroborated by previous SEC measurements. The steepness of the partitioning curves $K(\lambda)$ was related to the dependence of the free energy of confinement on the chain length $\Delta A(N)$. The 3D function $K(\lambda,\epsilon_w)$, universally describing the steric exclusion/adsorption partitioning, was constructed by fitting the simulation data. The 3D surface reproduces all regimes of nonideal partitioning including the critical chromatography. The free energy penalty $\Delta A/kT(\lambda)$ due to chain confinement, calculated for various concentrations and adsorption strengths, should ameliorate the estimations of this quantity in various polymer nanostructures under nonideal conditions. The molecular interpretation of the term $\Delta A/kT$ at nonideal partitioning, based on the loss of the conformational and orientational entropies of coils on their confinement, is discussed.

Acknowledgment. The research was supported in part by the Grant Agency for Science (VEGA), Grants 2/7056/20 and 2/7076/20. The use of computer resources of the Computing Centre of SAS is gratefully acknowledged.

References and Notes

(1) Teraoka, I. *Prog. Polym. Sci.* **1996**, *21*, 89.
(2) *J. Polym. Sci., Polym. Lett. Ed.* **1967**, *5*, 773.
(3) Casassa, E. F.; Tagami, Y. *Macromolecules* **1969**, *2*, 14.
(4) Hashimoto, T.; Shibayama, M.; Kawai, H.; Meier, D. J. *Macromolecules* **1985**, *18*, 1855.
(5) Tucker, P. S.; Paul, D. R. *Macromolecules* **1988**, *21*, 2801.
(6) Vaia, R. A.; Giannelis, E. P. *Macromolecules* **1997**, *30*, 7990.
(7) Davidson, M. G.; Suter, U. W.; Deen, W. M. *Macromolecules* **1987**, *20*, 1141.
(8) Cifra, P.; Bleha, T.; Romanov, A. *Polymer* **1988**, *29*, 1664.
(9) Gorbunov, A. A.; Skvortsov, A. M. *Adv. Colloid Interface Sci.* **1995**, *62*, 31.
(10) Skvortsov, A. M.; Gorbunov, A. A. *J. Chromatogr.* **1986**, *358*, 77.
(11) Lin, N. P.; Deen, W. N. *Macromolecules* **1990**, *23*, 2947.
(12) Satterfield, C. N.; Colton, C. K.; Turckheim, B. D.; Copeland, T. M. *AIChE J.* **1975**, *24*, 937.
(13) Brannon, J. H.; Anderson, J. L. *J. Polym. Sci., Polym. Phys. Ed.* **1982**, *20*, 857.
(14) Teraoka, I. *Macromolecules* **1996**, *29*, 2430.
(15) Cifra, P.; Bleha, T.; Romanov, A. *Macromol. Chem. Rapid Commun.* **1988**, *9*, 335.
(16) Bleha, T.; Cifra, P.; Karasz, F. E. *Polymer* **1990**, *31*, 1321.
(17) Wang, Y.; Teraoka, I. *Macromolecules* **1997**, *30*, 8473.
(18) Anderson, J. L.; Brannon, J. H. *J. Polym. Sci., Polym. Phys. Ed.* **1981**, *19*, 405.
(19) Teraoka, I.; Langley, K. H.; Karasz, F. E. *Macromolecules* **1993**, *26*, 287.
(20) Thompson, A. P.; Glandt, E. D. *Macromolecules* **1996**, *29*, 4314.
(21) Cifra, P.; Bleha, T. *Macromol. Theory Simul.* **1999**, *8*, 603.
(22) Cifra, P.; Bleha, T. *Macromol. Theory Simul.*, **2000**, *9*, 555.
(23) Cifra, P.; Bleha, T. *Polymer* **2000**, *41*, 1003.
(24) Dickman, R. *J. Chem Phys.* **1992**, *96*, 1516.
(25) Panagiotopoulos, A. Z.; Wong, V.; Floriano, M. A. *Macromolecules* **1998**, *31*, 912.
(26) Dayantis, J.; Sturm, J. *Polymer* **1985**, *26*, 1631.
(27) Giddings, J. C.; Kucera, E.; Russell, C. P.; Myers, M. N. *J. Phys. Chem.* **1968**, *72*, 4397.
(28) Daoud, M.; de Gennes, P.-G. *J. Phys (Paris)* **1977**, *38*, 85.
(29) de Gennes, P.-G. *Scaling Concepts in Polymer Physics*; Cornell University Press: Ithaca, NY, 1979.
(30) Berek, D.; Bakoš, D.; Bleha, T.; Šoltés, L. *Makromol. Chem.* **1975**, *176*, 391.
(31) Bleha, T.; Spychaj, T.; Vondra, R.; Berek, D. *J. Polym. Sci., Polym. Phys. Ed.* **1983**, *21*, 1903.
(32) Bleha, T.; Mlýnek, J.; Berek, D. *Polymer* **1980**, *21*, 798.
(33) Bezrukov, S. M.; Vodyanoy, I.; Brutyan, R. A.; Kasianowicz, J. J. *Macromolecules* **1996**, *29*, 8517.
(34) Berek, D. *Macromol. Symp.* **1996**, *110*, 33.
(35) Pasch, H. *Macromol. Symp.* **1996**, *110*, 107.
(36) Guttman, C. M.; DiMarzio, E. A.; Douglas, J. F. *Macromolecules* **1996**, *29*, 5723.
(37) Gorbunov, A. A.; Solovyova, L. Y.; Skvorcov, A. M. *Polymer* **1998**, *39*, 697.
(38) van Vliet, J. H.; Luyten, M. C.; ten Brinke, G. *Macromolecules* **1992**, *25*, 3802.
(39) Yethiraj, A. *J. Chem. Phys.* **1994**, *101*, 2489.
(40) Cifra, P.; Bleha, T., submitted to *Int. J. Polym. Anal. Charact.*

MA000964A